Supplementary Materials for

Identification of the Tau phosphorylation pattern that drives its aggregation.

Clément Despres, Cillian Byrne, Haoling Qi, François-Xavier Cantrelle, Isabelle Huvent, Béatrice Chambraud, Etienne-Emile Baulieu*, Yves Jacquot, Isabelle Landrieu, Guy Lippens,* Caroline Smet-Nocca*

correspondence to: glippens@insa-toulouse.fr; etienne.baulieu@inserm.fr; caroline.smet@univ-lille1.fr

This PDF file includes:

Materials and Methods
Figs. S1 to S14

Material and Methods

Peptide synthesis and purification

Peptides were synthesized manually using standard Fmoc-SPPS protocols, in a fritted syringe on a 0.1 mmol scale, using Rink amide resin (0.4 – 0.7 $mmol.g^{-1}$). Coupling was carried out using the requisite Fmoc protected amino-acids (10 eq.), O-(Benzotriazol-1-yl)-*N,N,N′,N′*-tetramethyluronium hexafluorophosphate (HBTU; 9.5 eq.), and *N,N*-Diisopropylethylamine (DIPEA; 20 eq.) with shaking for 1 h. Phosphorylated amino acids were double coupled (2 x 3 h) using protected phospho-amino acids (5 eq.), *N*-[(Dimethylamino)-1*H*-1,2,3-triazolo-[4,5-b]pyridin-1-ylmethylene]-*N*-methyl-methanaminium hexafluorophosphate *N*-oxide (HATU; 4.9 eq.) and DIPEA (15 eq.). After coupling, the resin was washed five times with NMP. Fmoc deprotection was carried out using 20 % piperidine in NMP (1 x 1 min, followed by 1 x 10 min.). After deprotection, the peptides were washed five times with NMP. Acetylation of the completed peptides was achieved using DIPEA (2 eq.) and $(Ac)_2O$ (15 eq.) in NMP. The completed peptides were washed successively in NMP (x 3), DCM (x3) and MeOH (x3), and then dried *in vacuo*. Concomitant cleavage from the resin and peptide deprotection was carried out using the cocktail TFA – iPr_3SiH (TIPS) – H_2O (95:2.5:2.5), approximately 10 $mL.g^{-1}$ of peptide resin, for 2 h. The suspension was filtered, the filtrate was evaporated to dryness *in vacuo*, and the residual material was triturated with ice-cold ether, centrifuged and the supernatant discarded (x 3), to furnish a white solid. The crude peptide products were dissolved in Milli-Q water and lyophilized before analysis and purification by Preparative RP-HPLC.

Peptide Purification/Analysis:

RP-HPLC was performed using a Waters 1525 binary pump system with a Waters 2487 dual wavelength absorbance detector and UV detection at 220 nm. Solvent A: 0.1% TFA in water and solvent B: 0.1% TFA in CH3CN. Analytical RP-HPLC was performed using a Higgins Analytical Proto200 C18 3 μM column (4.6 x 100 mm), at a flow rate of 1.0 $mL.min^{-1}$ with a gradient of 5 – 20% B in 10 min. Preparative RP-HPLC was performed using an Xbridge C18 5 μM (19 x 50 mm) column with a flow rate of 10 mL min-1 using the appropriate gradient. MALDI-TOF mass spectrometry analyses were performed in the ion positive reflector mode on an ABI Voyager DE-Pro MALDI-TOF mass spectrometer (Applied Biosystems) using as matrix a saturated solution of α-cyano-4-hydroxycinnamic acid (CHCA) in CH_3CN:H_2O:CF_3COOH (50:50:0.1).

The synthesis of peptides **0P-AT8** and **2P-AT8** has been described previously.[1]

Ac-GDRSGYSSPGSPGTPGSRSRT-*NH2*.(3TFA) **Peptide 0P-AT8**

Ac-GDRSGYSSPG(pS)PG(pT)PGSRSRT-*NH2*.(3TFA) **Peptide 2P-AT8**

Ac-GDRSGYSSPGSPGTPVSRSRT-*NH2*.(3TFA) **Peptide 0P-AT8-G207V**

Preparative HPLC (Xbridge C_{18} 9-15%B over 10 min) *R*T = 7.32 min. Analytical HPLC (PROTO200 C_{18} 5–20% B over 10 min) *R*T = 9.69 min. MALDI-TOF $[M+H]^+$ *m/z* : 2149.1996 (calc. 2149.0386).

Ac-GDRSGYSSPG(pS)PG(pT)PVSRSRT-*NH2*.(3TFA) **Peptide 2P-AT8-G207V**

Preparative HPLC (Xbridge C_{18} 7-17%B over 10 min) *R*T = 7.20 min. Analytical HPLC (PROTO200 C_{18} 5–20% B over 10 min) *R*T = 8.32 min. MALDI-TOF $[M+H]^+$ *m/z* : 2309.1191 (calc. 2308.97).

Ac-GDRSGYSSPG(pS)PG(pT)PG(pS)RSRT-*NH2*.(3TFA) **Peptide 3P-AT8**

Preparative HPLC (Xbridge C_{18} 5-20%B over 10 min) *R*T = 5.43 min. Analytical HPLC (PROTO200 C_{18} 5–20% B over 10 min) *R*T = 6.95 min. MALDI-TOF $[M+H]^+$ *m/z* : 2346.45 (calc. 2346.89).

Production of ^{15}N- and ^{13}C-labeled Tau441 and TauF8 fragment in *Escherichia Coli*

The Tau441 (residues 1-441 of human MAPT) and TauF8 fragments (residues 192-324) in their wild-type or mutant forms (G207V or S262A) were produced in the *E. coli* BL21 DE3 strain carrying in the pET15b recombinant plasmid (Novagen). Cells were grown at 37°C in M9 minimal medium containing 2g/l $^{13}C_6$-glucose, 1g/l ^{15}N-ammonium chloride, 0,5 g/l ^{15}N,^{13}C-Isogro® (Sigma), 1mM $MgSO_4$, 100µM $CaCl_2$, MEM vitamins cocktail (Sigma) and ampicillin (100mg/l). When the OD at 600nm reached 0.8, the induction phase was initiated by addition of 0.5mM IPTG and continued for 3h at 37°C. Cells were harvested by centrifugation at 4000×g for 25 min and the pellet was resuspended in 50mM NaH_2PO_4/Na_2HPO_4 (pH 6.2), 2.5mM EDTA, 2mM DTT and 0.5% triton X100 complemented with a protease cocktail inhibitor (Complete^{TM}, Roche). The lysate was obtained by homogenization of this suspension with a high-pressure homogenizer (Emulsiflex, Avestin) followed by centrifugation at 30,000×g for 30 min. The soluble extract was incubated at 75°C for 15 min. The soluble proteins were isolated by centrifugation at 30,000×g for 30 min and purified by cation exchange chromatography (HiTrap SP HP 1ml, GE Healthcare). Then, fractions were checked by SDS-PAGE (T=12% for full length Tau and 15% for TauF8) and pooled for buffer-exchange in

50mM ammonium bicarbonate prior to lyophilization. Lyophilized proteins were kept at -20°C until further use.

In vitro phosphorylation of Tau and TauF8 fragments by ERK2

100µM of $^{15}N,^{13}C$ Tau or TauF8 (wild type or mutant forms) was mixed with 1µM of ERK2 and about 0.1µM of MEK R_4F (MEK3), the constitutively active mutated form of MEK3. The mixture was incubated at 37°C overnight in 400µl of phosphorylation buffer (50mM Hepes.KOH pH8.0, 12.5mM $MgCl_2$, 50mM NaCl, 2mM EDTA, 1mM DTT, 1mM EGTA, 12.5mM ATP). Enzymatic reaction was stopped by heating the reaction mixture at 75°C for 15 min followed by centrifugation 16,000×g for 20 min. Then, the supernatant was buffer-exchanged in 50mM ammonium bicarbonate prior to lyophilization. Prior to further analyses, a gel shift of protein band on SDS-PAGE (T=10% for *p*-Tau441 and T=12% for *p*-TauF8) allowed a qualitative control of protein phosphorylation. A control experiment was performed under the same conditions in which ERK2 was omitted. The absence of phosphorylation detected by NMR indicates that MEK R_4F does not directly phosphorylate Tau. Each set of phosphorylation experiment was independently repeated three times with new batches of Tau proteins and kinases.

In vitro phosphorylation of Tau and TauF8 fragments by rat brain extract (RBE)

The rat brain extract (RBE) was prepared from adult rat Sprague-Dawley by homogenizing a brain (about 2g) in 5ml of homogenizing buffer (10mM Tris pH7.4, 5mM EGTA, 2mM DTT, 1µM okadaic acid (Sigma)) supplemented with 20µg/ml Leupeptin and 40mM Pefabloc. Ultracentrifugation was performed at 100,000×g at 4°C for 1hr. The supernatant was directly used for its kinase activity. Total protein concentration was estimated at 11mg/ml by BCA colorimetric assay (Pierce). The $^{15}N,^{13}C$ Tau and TauF8 fragments, in their wild type or mutants forms, were dissolved respectively at 10 and 25µM in 2.5ml of phosphorylation buffer (40mM Hepes pH7.3, 2mM $MgCl_2$, 5mM EGTA, 2mM DTT, 2mM ATP and 1 µM okadaic acid) complemented with a protease inhibitor cocktail (Complete^{TM}, Roche). The phosphorylation reaction was performed at 37°C for 24hr with 500µl of brain extract. Enzymatic reaction was stopped by heating the mixture at 75°C for 15 min and centrifugation at 16,000×g for 20 min. Then, the supernatant was buffer-exchanged in 50mM ammonium bicarbonate prior to lyophilization. Qualitative control of protein phosphorylation was performed by SDS-PAGE prior to NMR analyses and aggregation assays. Each set of phosphorylation experiment was independently repeated three times with new batches of Tau proteins and fresh rat brain extract.

NMR spectroscopy

NMR of peptides was performed on 800 or 900MHz Bruker spectrometers equipped with a triple resonance cryogenic probe head. Homonuclear Nuclear Overhauser (NOESY) and Total Correlation (TOCSY) spectra were acquired at 293K with standard pulse programs on 2mM peptide samples in a phosphate buffer (50mM phosphate buffer pH 6.4, 25mM NaCl, 2,5mM

EDTA, and 5% D_2O). ^{1}H, ^{15}N Heteronuclear Single Quantum (HSQC) spectra were acquired at natural abundance, with 128scans per increment and 2048x256 complex points in the t_2 and t_1 directions, respectively. Peptide NMR spectra were processed in Topspin3.0, and manually assigned.

For protein NMR experiments, 5mm closed SHIGEMI tubes were used. All spectra were acquired at 293K on a Bruker 900MHz spectrometer equipped with a triple resonance cryogenic probehead. Tau proteins were dissolved at a concentration of 200-300µM in NMR sample buffer (50mM phosphate buffer pH 6.4, 25mM NaCl, 2,5mM EDTA, 1mM DTT and 10% D_2O). The proton frequency was calibrated with 1mM TMSP as a reference. ^{1}H-^{15}N HSQC were recorded on ^{15}N- and ^{15}N,^{13}C-labeled samples with 64 scans per increment, and 3072 and 512 points in proton and nitrogen dimensions, respectively (experiment time 11.25hr).

For TauF8 and *p*-TauF8 wild-type assignment, ^{15}N,^{13}C-labeled proteins were used and 3D experiments HN(CO)CACB and HNCACB experiments were performed with 16 scans per increment. Spectral widths were 16.0, 23.0 and 61.0 ppm in ^{1}H,^{15}N and ^{13}C dimensions, respectively, with 2048, 64 and 120 sample points.

Spectra were processed with Bruker Topspin 3.5pl2 software. Data analysis, peak picking and calculation of peak volumes were done with the computer program NMRFAM-SPARKY (https://www.cgl.ucsf.edu/home/sparky). . To estimate phosphorylation levels at each site, the ratio of the peak integral corresponding to phosphorylated forms over the sum of peak integrals corresponding to non-phosphorylated and phosphorylated forms were calculated.

In vitro aggregation assay and transmission electron microscopy (TEM)

Tau aggregation assays were performed at 10µM of Tau441 wild-type or S262A phosphorylated by rat brain extract in aggregation buffer (100mM MES buffer pH6.9, 2mM EGTA, 1mM $MgCl_2$, 0.33mM DTT and 50µM Thioflavin T). Lyophilized proteins were resuspended in the aggregation buffer at the desired concentration and 50µM ThT was added. Aggregation kinetics were followed by ThT emission at 490nm using a plate reader (PHERAStar, BMG Labtech). In parallel, aggregation experiments were performed under the same conditions in 1.5ml tubes. Mixtures were incubated for 5 days at 37°C without agitation. At the end of incubation, 10µl samples from 1.5ml tubes and plates were withdrawn and applied on 400-mesh hexagonal formvar-coated grids for 90 sec. The sample-loaded grids were washed three times with ultrapure water and drained. The grids were next negatively stained with 2% uranyl-acetate solution for 90 sec and washed two times with ultrapure water. Transmission electron microscopy was performed with a HITACHI H7500 microscope at 80kV.

Immunogold TEM. For immunogold labeling of the fibrils, 10 µL of the aggregation sample was adsorbed on carbon-coated EM grids (Electron Microscopy Science) for 20 min. Excess fibrils were removed by placing the EM grids three times on drops of fresh PBS buffer without drying. After blocking in 1% (wt/vol) BSA in PBS for 60 min, grids were incubated with primary anti-Tau antibody (Human PHF-TAU clone AT8 or anti-Tau (4-repeat isoform RD4), clone 1E1/A6) diluted 1:100 in 1% BSA for 1 h. After further washing the grids five times in PBS, they were incubated with the gold-labeled secondary antibody (6nm-Glod donkey IGG

anti-mouseIGG (H+L)) diluted 1:20 in 1% BSA for 60 min, followed by five washes in PBS. Before staining, the sample was washed 10 times in water to avoid precipitation of uranyl-acetate in PBS. The sample was negatively stained by incubation in 2% (wt/ vol) uranyl-acetate in water for 8 min, followed by 4 washing/drying steps in water. Transmission electron microscopy was performed with a HITACHI H7500 microscope at 80kV.

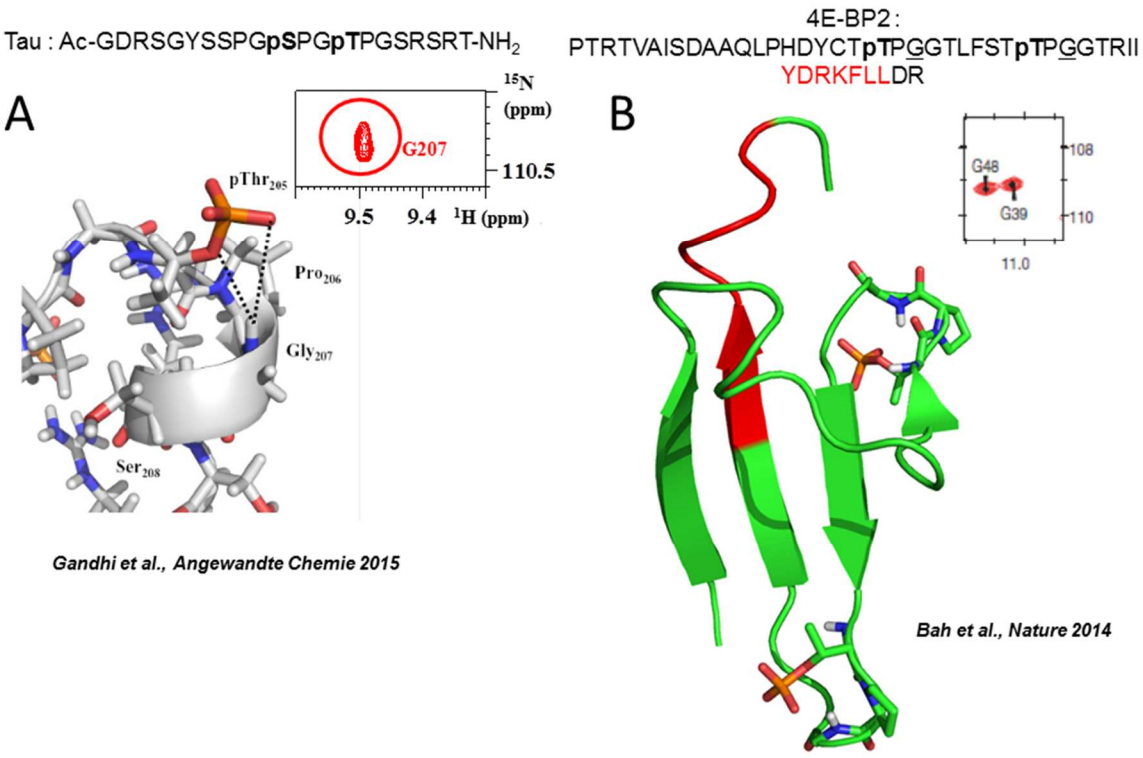

Figure S1 : (A) The helical turn induced by the phosphorylation of Ser202 and Thr205 in the 2P-AT8 peptide is populated half of the time, and leads to a chemical shift of 9.5ppm for the amide proton of Gly207 (*1*). **(B)** In contrast, the phosphorylation-induced TPG turns in 4E-BP2 (at pT37/pT46) lead to a stable folding of the latter into a four-stranded β-sheet with concomitant amide proton chemical shift values of 11ppm for Gly39 and Gly48 (*2*). The β-sheet hides the eIF4E interacting peptide (in red) in a first example of anti-structural biology (*3*).

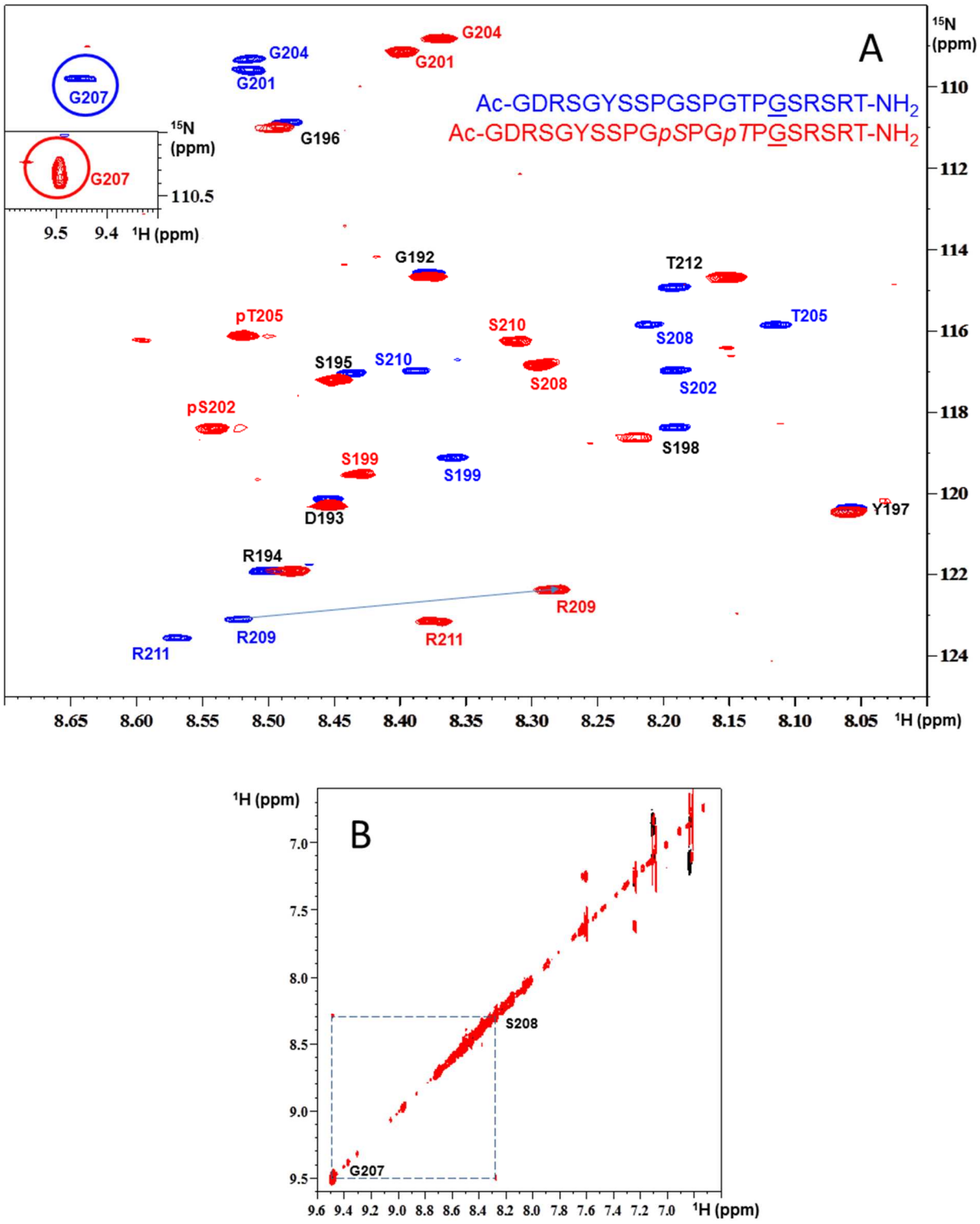

Figure S2 : (A) $^{1}H,^{15}N$ HSQC spectra of the non-phosphorylated (0P-AT8; blue) and doubly phosphorylated (2P-AT8; red) peptides of Tau. Phosphorylation of Ser202 and Thr205 in the latter causes a 0.9ppm chemical shift for the amide proton of Gly207, and substantial shifts for the amide protons of Arg209 and Arg211. **(B)** Zoom of the amide proton region of the NOESY spectrum of the 2P-AT8 peptide, showing the H_N-H_N cross peak between the amide protons of Gly207 and Ser208, indicative of the turn conformation (*1*).

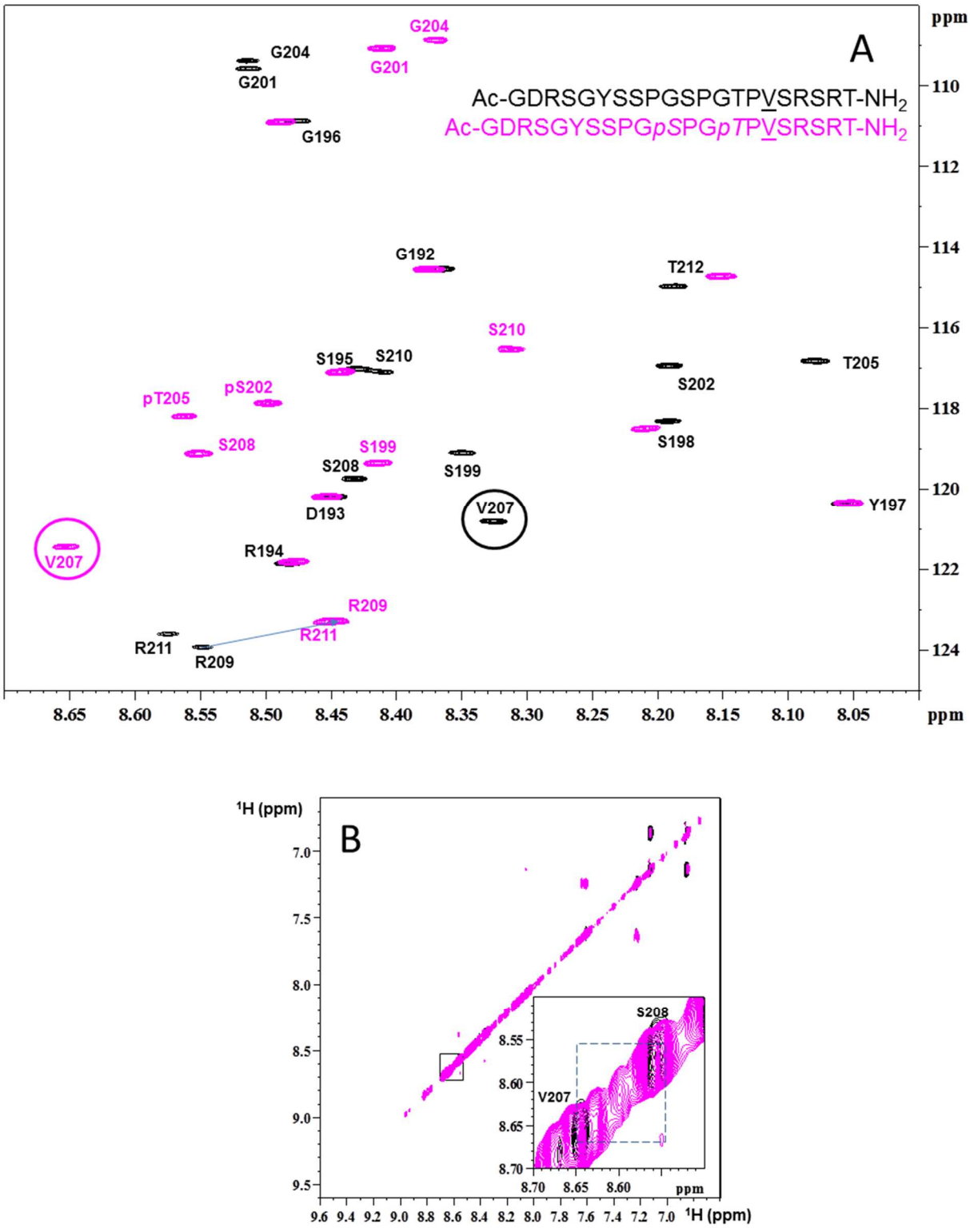

Figure S3 : (A) $^{1}H,^{15}N$ HSQC spectra of the non-phosphorylated (0P-AT8-G207V; black) and doubly phosphorylated (2P-AT8-G207V; magenta) peptides of Tau carrying the Gly207Val substitution. Phosphorylation of Ser202 and Thr205 in the latter has more limited consequences than for the 2P-AT8 peptide, with a mere 0.3ppm chemical shift for the amide proton of Val207, and reduced shifts for the amide protons of Arg209 and Arg211. **(B)** Zoom of the amide proton region of the NOESY spectrum of the 2P-AT8-G207V peptide, showing the absence of a H_N-H_N cross peak between the amide protons of Val207 and Ser208. As in 4E-BP2 (*2*), the Gly-to-Val substitution hinders the helical turn conformation.

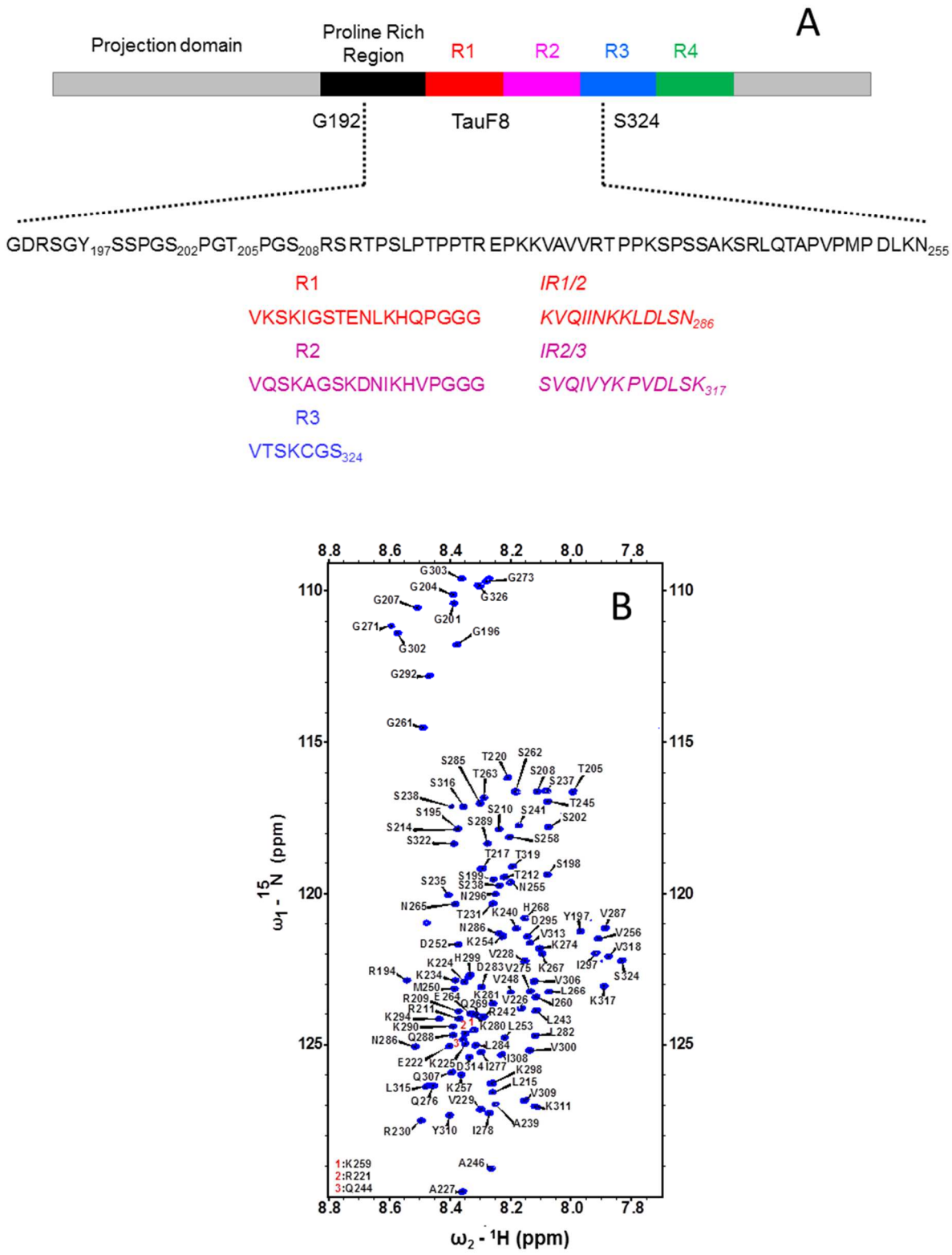

Figure S4 : (A) Primary sequence of TauF8, spanning the sequence of Gly192 to Ser324 of the longest Tau441 isoform. TauF8 carries the C291A mutation, leaving a single cysteine residue at position 322. **(B)** Assigned ^{1}H-^{15}N HSQC spectra of TauF8.

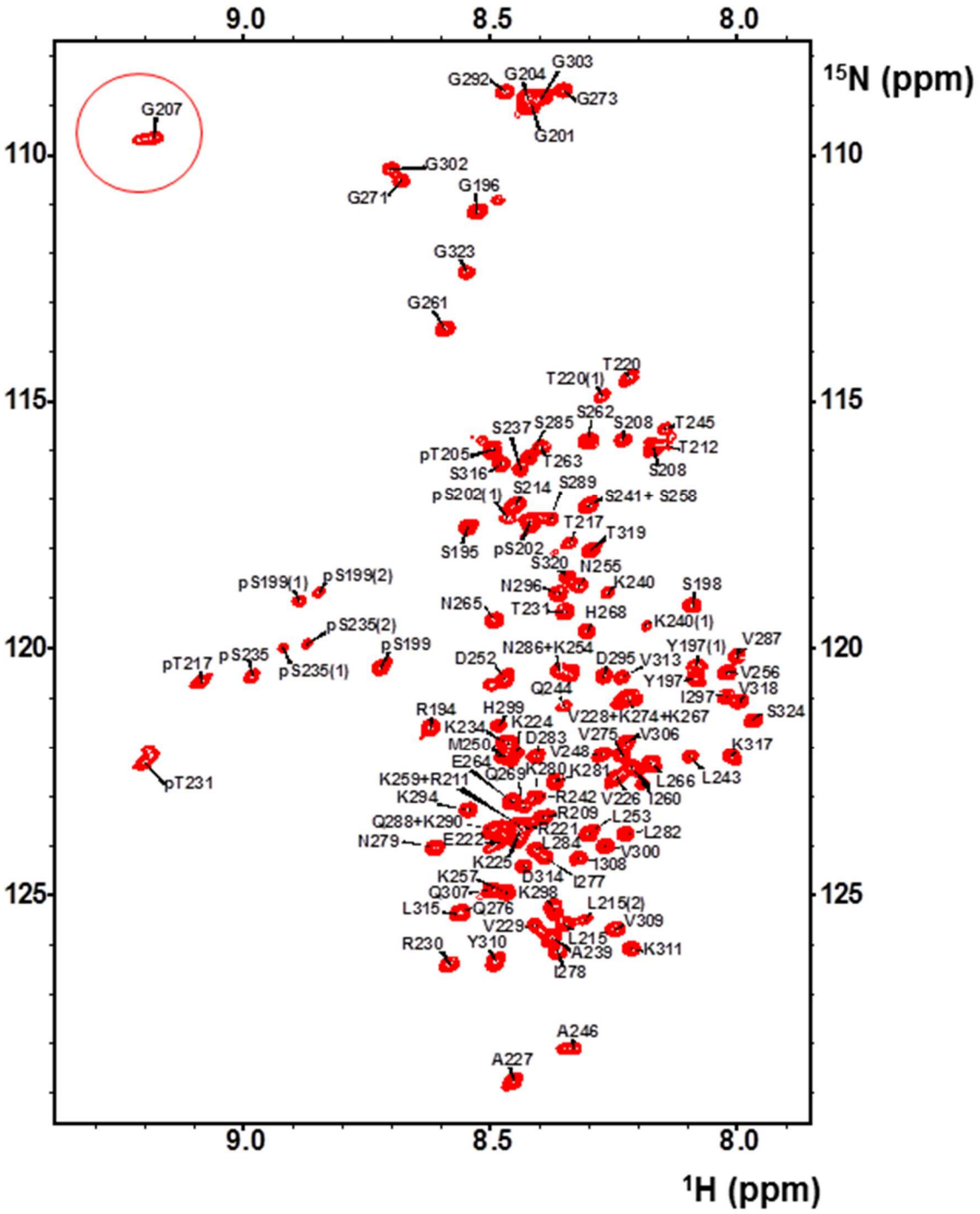

Figure S5 : ^{1}H-^{15}N HSQC spectra of TauF8 phosphorylated by ERK2. Assignment of the ERK2-phosphorylated TauF8-C291A fragment was performed by using classical 3D NMR experiments, HNCACB and HN(CO)CACB, on ^{15}N,^{13}C-labeled sample at 900MHz. Six phosphorylated Thr/Ser-Pro motifs (pS199, pS202, pThr205, pThr217, pThr231, pSer235) are identified in the region from 8.7 to 9.3ppm (^{1}H) which is empty in the spectrum of the non-phosphorylated fragment. Downfield shift of the Gly207 amide proton indicates that phosphorylation by ERK2 induces the turn-like structure of the AT8 epitope (*1*).

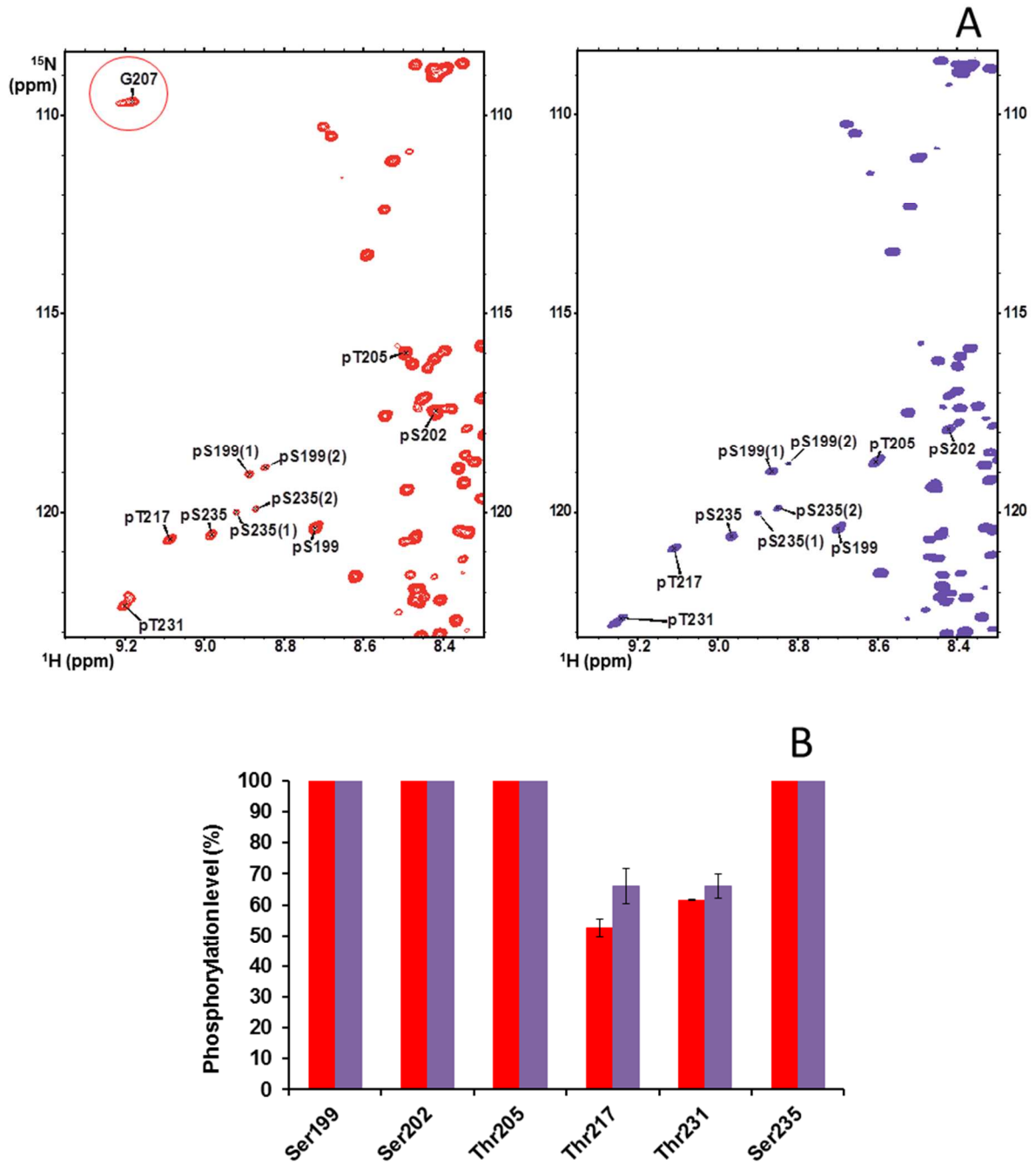

Figure S6 : (A) Zoom of the ^{1}H-^{15}N HSQC spectra centered on the resonances of the phosphorylated residues of TauF8 (red) or TauF8-G207V (purple) phosphorylated by ERK2. The G207V mutation in TauF8 does not change qualitatively the phosphorylation pattern as assessed by NMR. We note that pThr205 is more downfield shifted in the ERK2 phosphorylated TauF8-G207V sample pointing towards a more pronounced intra-residue hydrogen bonding between the phosphate group and its own amide proton. **(B)** Measurement of phosphorylation levels at each site in both samples confirms that phosphorylation patterns are also quantitatively similar. Ser202 and Thr205 were quantitatively phosphorylated in both samples. Phosphorylation by ERK2 was independently repeated three times, standard deviation around average value is shown by error bars. Levels of phosphorylation are estimated based on the integrals of resonance peaks as described in methods (NMR spectroscopy).

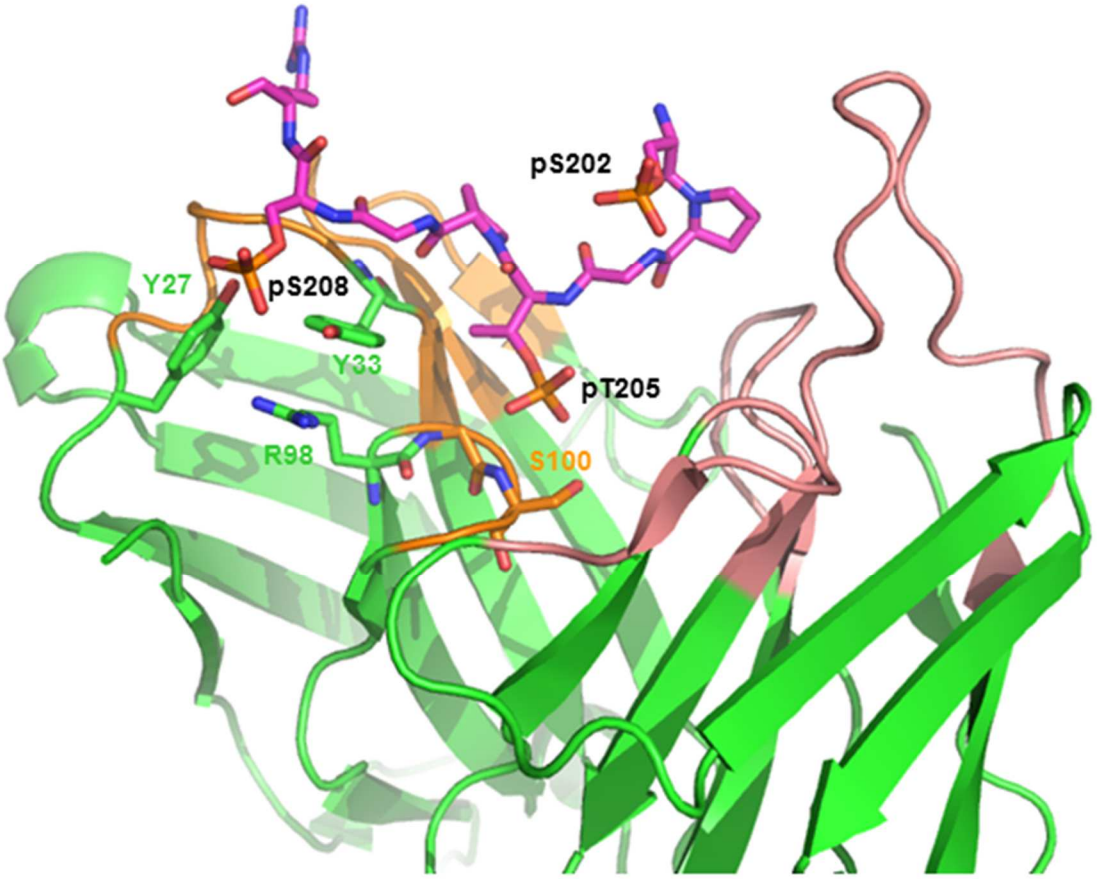

Malia et al., Proteins 2016

Ac-GDRSGYSSPG**pS**$_{202}$PG**pT**$_{205}$PG**pS**$_{208}$RSRT-NH_2

Figure S7 : Crystal structure of the AT8 Fab fragment in complex with a triply phosphorylated Tau peptide (PDB ID: 5E2W) The peptide binds to the clinical antibody in an extended conformation, and the additional phosphorylation of Ser208 leads to a tenfold improvement in binding affinity (*4*).

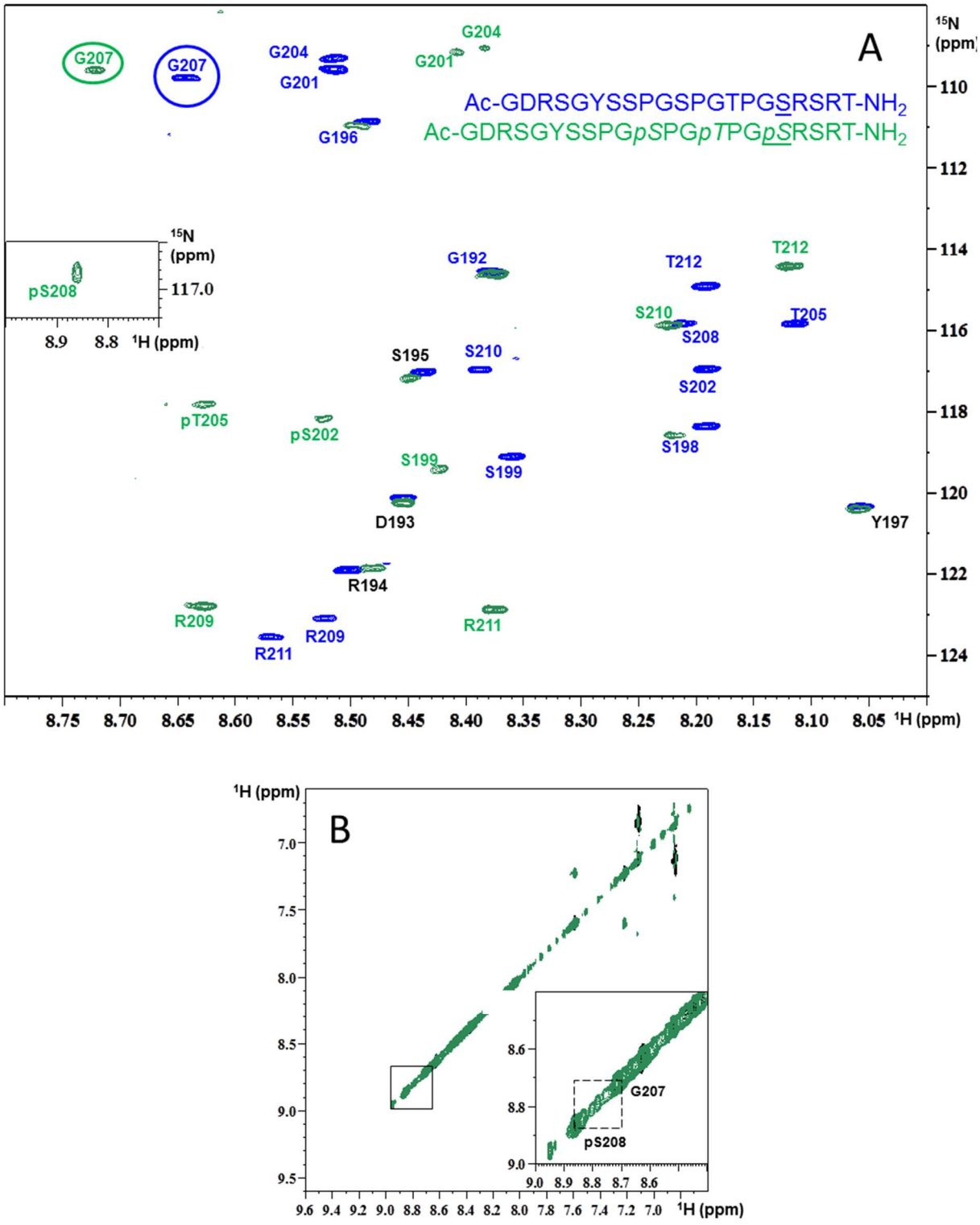

Figure S8 : (A) ^{1}H, ^{15}N HSQC spectra of the non-phosphorylated (0P-AT8; blue) and triply phosphorylated (3P-AT8; green) peptides of Tau. Additional phosphorylation of Ser208 (on top of the phosphorylation of Ser202 and Thr205 already present in 2P-AT8) eliminates the 0.9ppm chemical shift perturbation of Gly207 seen in 2P-AT8, and equally inverses the shift for the amide proton of Arg209. **(B)** Zoom of the amide proton region of the NOESY spectrum of the 3P-AT8 peptide, showing the absence of a H_N-H_N cross peak between the amide protons of Gly207 and Ser208. As for the Gly-to-Val substitution, the additional phosphorylation of Ser208 hinders the helical turn conformation.

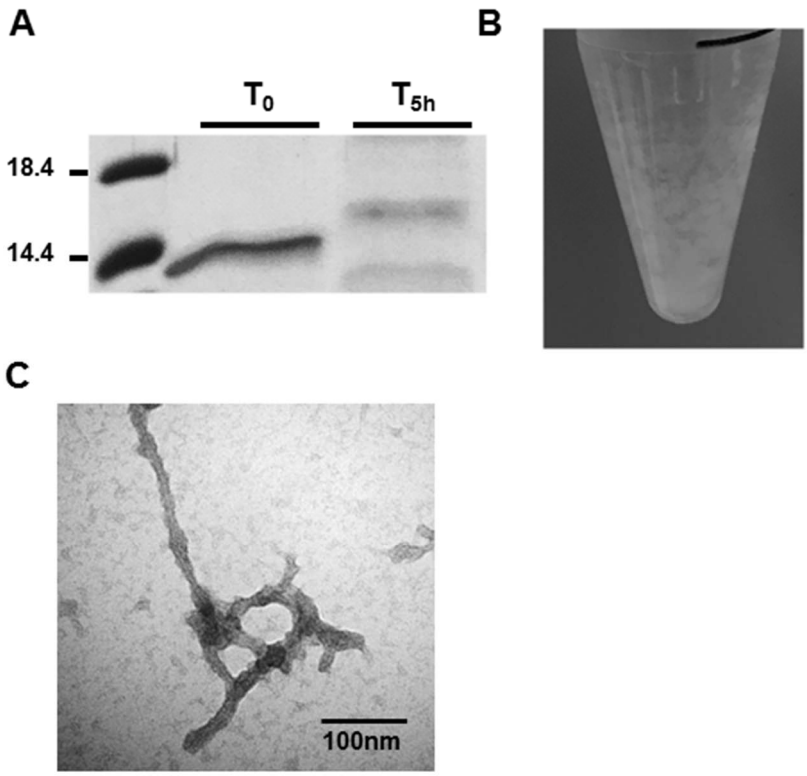

Figure S9 : Aggregation of TauF8-S262A during the RBE catalyzed phosphorylation reaction. **(A)** SDS-PAGE analysis (T=12%) of TauF8-S262A before and after 5h of reaction with RBE. After 5h of incubation, we observe a quasi-total loss of the soluble fraction. **(B)** Pellet observed after 5h of incubation in a 15ml tube. **(C)** Negative-staining Electron Microscopy (EM) of the pellet after 5h of incubation with RBE confirms the aggregation of TauF8-S262A during the phosphorylation reaction with RBE.

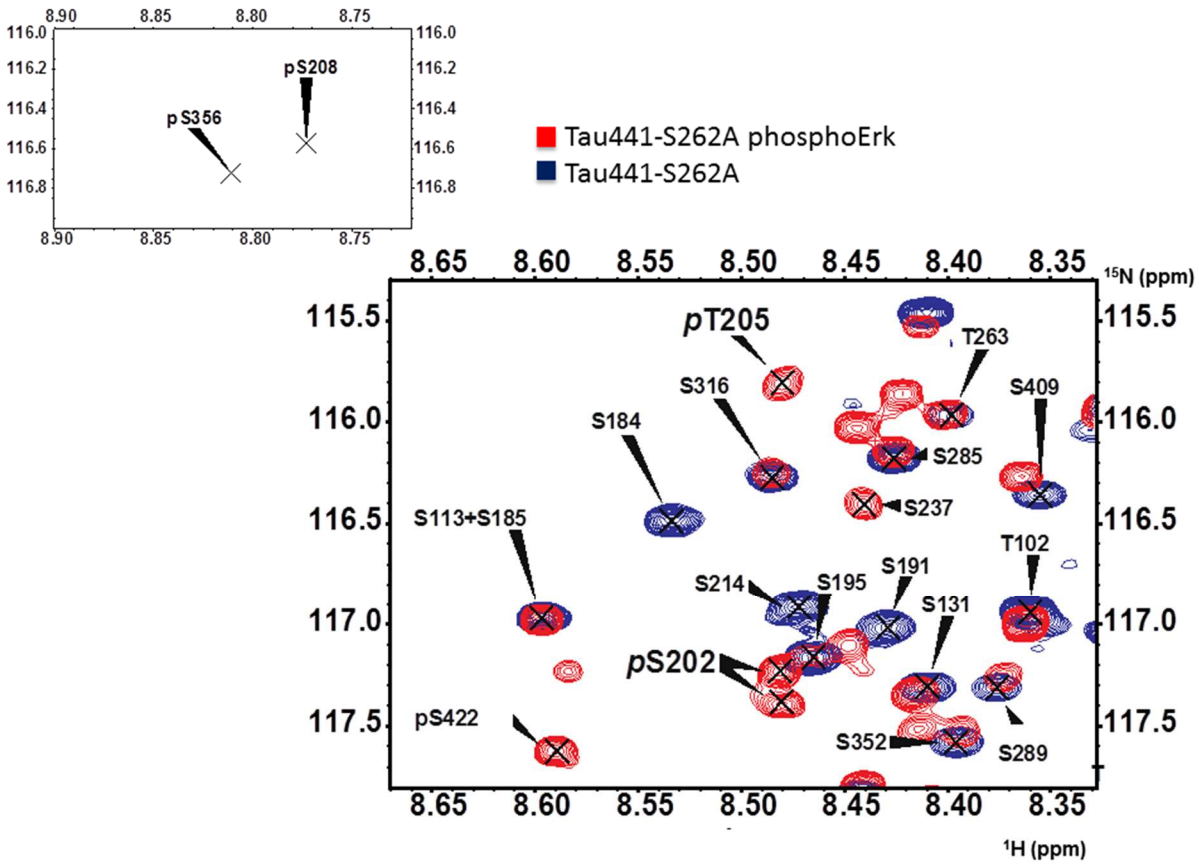

Figure S10 : Overlay of the ^{1}H-^{15}N HSQC spectra of Tau441-S262A before (blue) or after (red) phosphorylation by ERK2. Both Ser202 and Thr205 are fully phosphorylated by the activated ERK2 kinase. As ERK2 is a proline directed kinase, the region where we would expect resonances for phosphorylated Ser356 and Ser208 (see Figure S11) is empty.

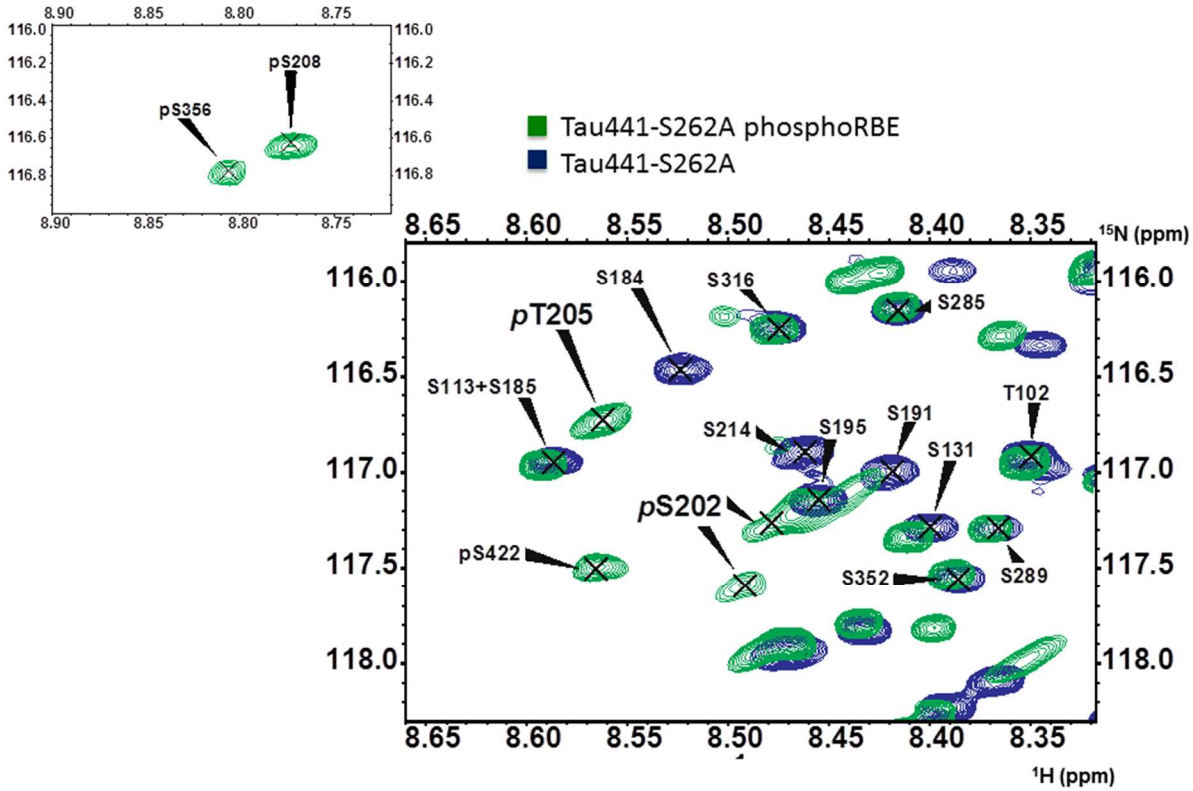

Figure S11 : Overlay of the ^{1}H-^{15}N HSQC spectra of Tau441-S262A before (blue) or after (green) phosphorylation by the RBE. Both Ser202 and Thr205 are fully phosphorylated by the kinase activity of the RBE. However, the RBE does contain additional non-proline directed kinase(s), so we can observe phosphorylated Ser356 and Ser208 resonances.

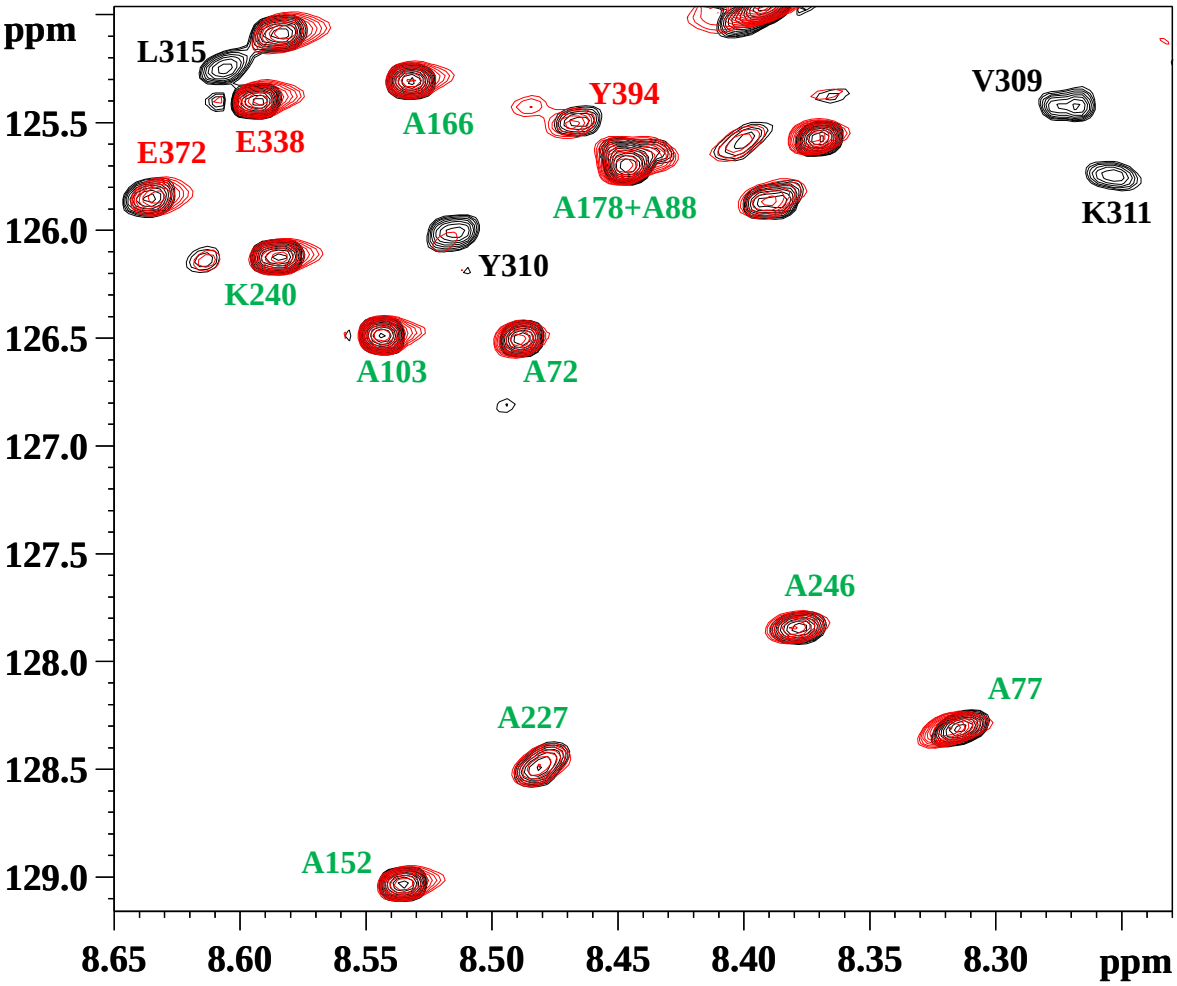

Figure S12 : Overlay of the ^{1}H-^{15}N HSQC spectra of Tau441-S262A phosphorylated by RBE before (black) or after (red) aggregation for 7 days at 37°C. The spectra are recorded at 20°C but directly in the MES aggregation buffer. Signals of residues in the repeat region, and notably the PHF6 peptide (annotated in black) loose intensity as they are integrated in the rigid core of the fibers, whereas signals of residues in the N- (green annotations) and C-termini (red annotations) of Tau maintain significant intensity because of their residual mobility.

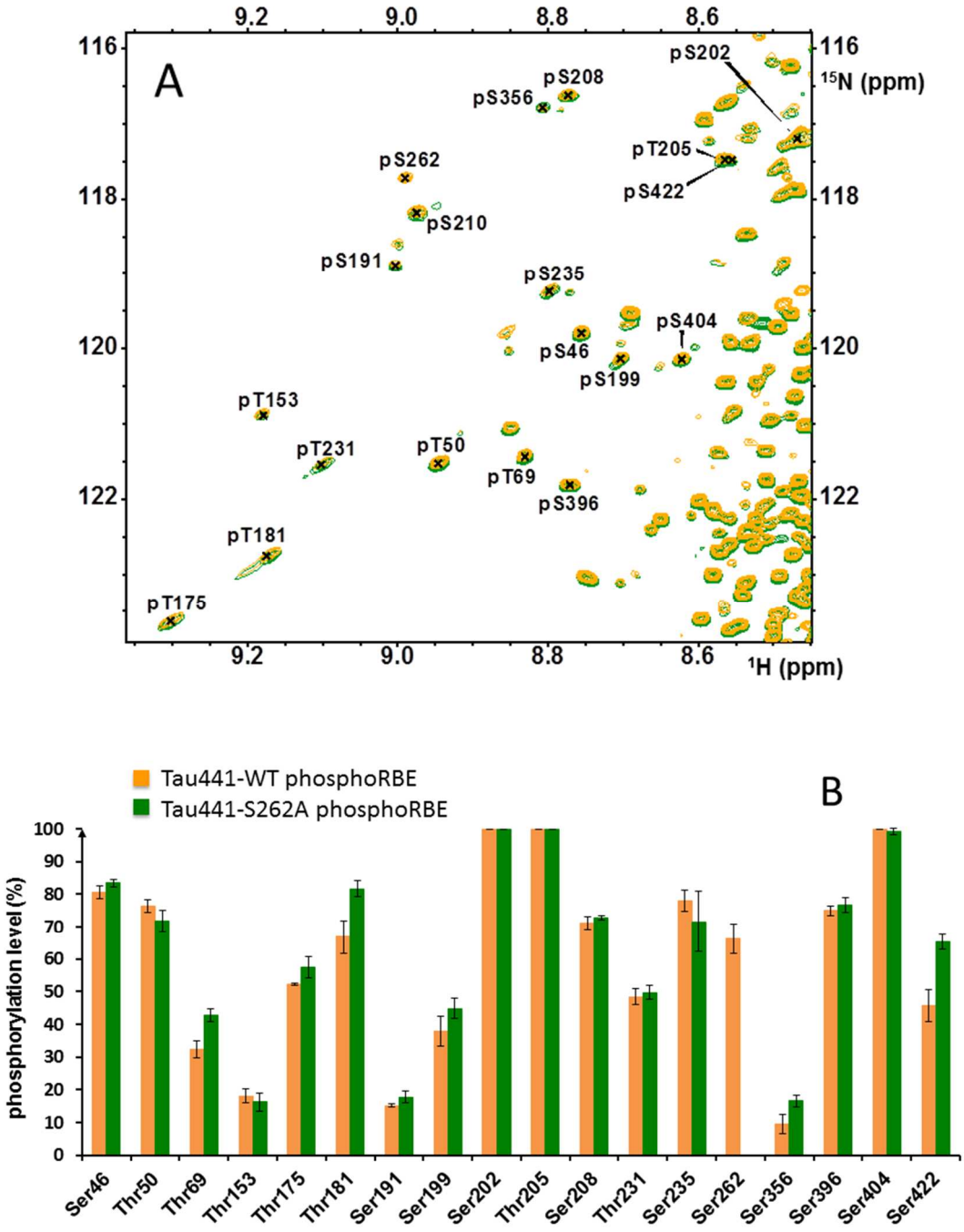

Figure S13 : (A) Zoom of the ^{1}H-^{15}N HSQC spectra centered on the resonances of the phosphorylated residues of Tau441-S262A (green) or wt Tau441 (orange) phosphorylated by the RBE. The S262A mutation in Tau441 does not change qualitatively the phosphorylation pattern as assessed by NMR. **(B)** Measurement in both samples of the levels of phosphorylation at each site confirms that phosphorylation patterns are also quantitatively similar. Phosphorylation of the Ser262 position in wt Tau441 is roughly 70%, whereas it is evidently absent in the Tau441 S262A mutant. Phosphorylation by fresh rat brain extract was independently repeated three times, standard deviation around average value is shown by error bars. Levels of phosphorylation are estimated based on the integrals of resonance peaks as described in methods (NMR spectroscopy).

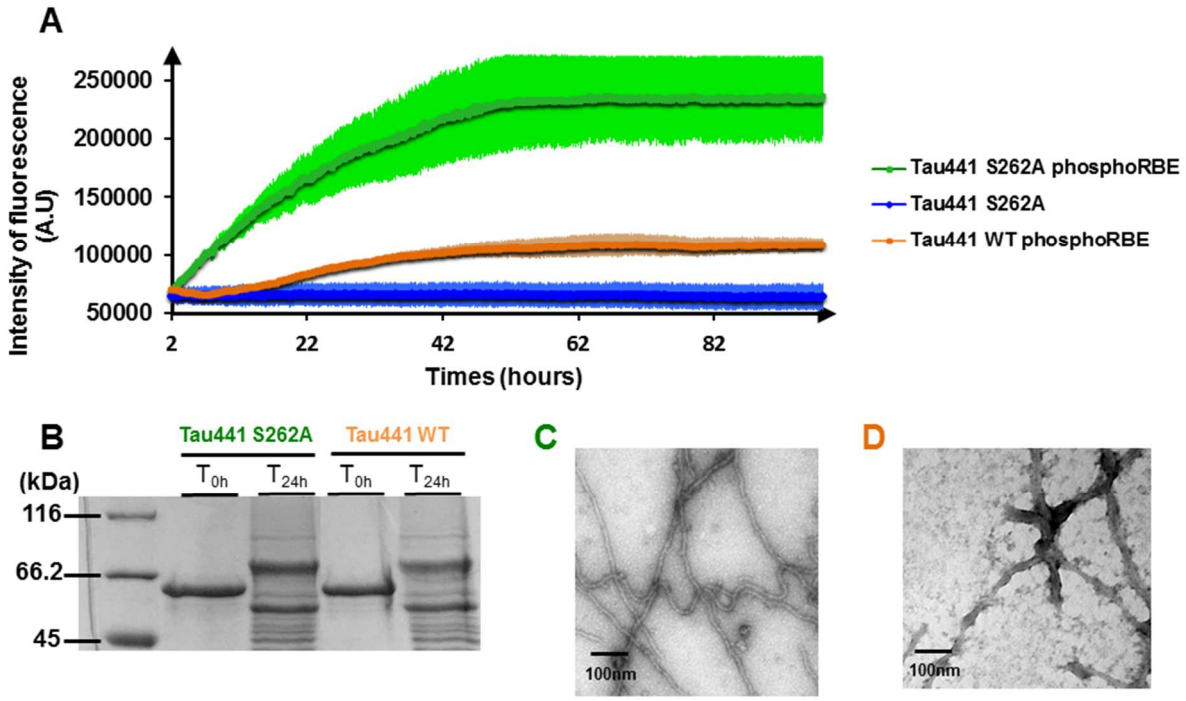

Figure S14 : Confirmation of the inhibitory role of Ser262 phosphorylation in a heparin-free aggregation assay. **(A)** Aggregation of Tau441-S262A (blue), Tau441-S262A phosphorylated by RBE (green) and Tau441-wt phosphorylated by RBE (orange) as followed by ThT emission at 490nm. A robust increase of ThT emission at 490nm is observed for the phosphorylated Tau441-S262A sample, but we equally observe a weaker signal for RBE-phosphorylated wt Tau441. We tentatively assign this signal to the 30% fraction of wt Tau441 that was not phosphorylated atSer262 after incubation with RBE (see Figure S12). **(B)** SDS-PAGE (T=10%) analysis of wt Tau441 and Tau441-S262A before (T_{0h}) and after phosphorylation by RBE (T_{24h}). After 24h of incubation with RBE, both samples display the characteristic gel shift. **(C, D)** Negative-staining EM at the end point of the aggregation assay of Tau441-S262A and wt Tau441, both phosphorylated by RBE. The amount of fibers observed for the RBE-phosphorylated Tau441-S262A was superior to that observed for the RBE-phosphorylated wt Tau441. Aggregation assay was independently repeated three times, standard deviation around average value is shown by error bars. For each experiment, triplicate analysis was done.

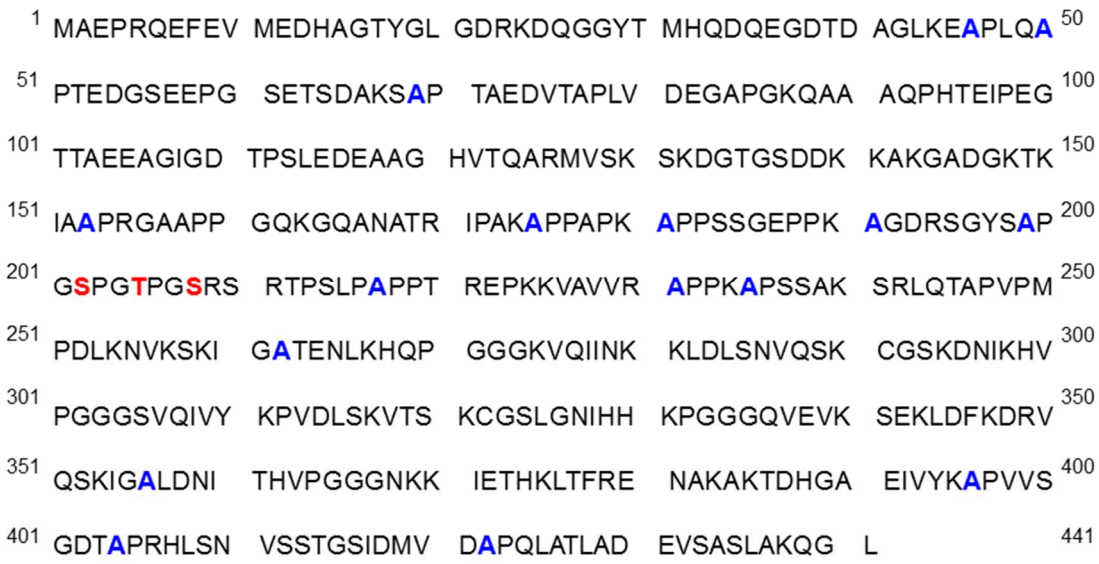

Figure S15 : Primary sequence of the Tau441-AT8 protein. The RBE phosphorylated residues as identified by NMR analysis of the phosphorylated Tau441 sample (Figure S12) were all mutated to Ala, except for the Ser202/Thr205/Ser208 residues corresponding to the 3P-AT8 epitope.

References

1. N. S. Gandhi *et al.*, A Phosphorylation-Induced Turn Defines the Alzheimer's Disease AT8 Antibody Epitope on the Tau Protein. *Angew. Chem. Int. Ed. Engl.* (2015), doi:10.1002/anie.201501898.

2. A. Bah *et al.*, Folding of an intrinsically disordered protein by phosphorylation as a regulatory switch. *Nature*. **519**, 106–109 (2015).

3. G. Bouvignies, M. Blackledge, Structural biology turned on its head. *Chembiochem*. **16**, 1033–1034 (2015).

4. T. J. Malia *et al.*, Epitope mapping and structural basis for the recognition of phosphorylated tau by the anti-tau antibody AT8. *Proteins* (2016), doi:10.1002/prot.24988.